Article

Discovery Medicine 2026; 38(214): 3756–3768
https://doi.org/10.24976/Discov.Med.202638214.285

Overcoming Oxaliplatin Resistance in Colorectal Cancer: Bioinformatics Identifies AKAP12 as a Functional Target of IL-24

Zejun Fang[1,2], Yanyan Hu[1,2], Minjing Zhu[1,2], Hengming Mei[1,2], Chaoju Gong[3,*], Wanshuang Lou[4,5,*]

[1]Central Laboratory, Sanmen People's Hospital, 317100 Taizhou, Zhejiang, China
[2]Central Laboratory, Sanmenwan Branch, The First Affiliated Hospital, Zhejiang University School of Medicine, 317100 Taizhou, Zhejiang, China
[3]Central Laboratory, The Affiliated Xuzhou Municipal Hospital of Xuzhou Medical University, 221100 Xuzhou, Jiangsu, China
[4]Department of Integrated Traditional & Western Medicine, Sanmen People's Hospital, 317100 Taizhou, Zhejiang, China
[5]Department of Integrated Traditional & Western Medicine, Sanmenwan Branch, The First Affiliated Hospital, Zhejiang University School of Medicine, 317100 Taizhou, Zhejiang, China
*Correspondence: gongcj@zju.edu.cn (Chaoju Gong); louwanshuang@zjsmyy.com (Wanshuang Lou)
Submitted: 23 July 2026 Revised: 17 September 2026 Accepted: 14 October 2026 Published: 25 November 2026

Background: The role of interleukin-24 (IL-24) in oxaliplatin resistance in colorectal cancer remains unclear, although its broader tumor-inhibitory effects are well established. This study aims to explore the role of IL-24 in oxaliplatin resistance in colorectal cancer.

Methods: Survival analyses were performed using the Kaplan-Meier methodology. Key cellular functions were evaluated using multiple experimental techniques, including Annexin V-fluorescein isothiocyanate (FITC)/propidium iodide (PI) staining, colony formation and cell counting kit-8. Differentially expressed genes retrieved from the GSE42387 and GSE76092 datasets were used as the basis for developing a prognostic signature using Least Absolute Shrinkage and Selection Operator (LASSO) regression analysis. The oxaliplatin-resistant SW480-OxR cell line was established. JC-1 staining to assess mitochondrial membrane potential (MMP) and measurement of cellular adenosine triphosphate (ATP) levels were used to evaluate mitochondrial function.

Results: In an exploratory analysis of rectal adenocarcinoma (READ) and colon adenocarcinoma (COAD) tissues from the UALCAN database, IL-24 expression was elevated compared with normal tissues ($p < 0.001$). Compared with the NCM460 cells, IL-24 expression was significantly elevated in SW480 cells ($p < 0.01$). Reduced IL-24 expression was associated with a poorer survival trend in READ patients, but the difference was not statistically significant ($p = 0.08$); no significant association was observed in COAD patients ($p = 0.86$). IL-24 overexpression suppressed proliferation and induced apoptosis in SW480 cells ($p < 0.05$). Subsequently, based on the prognostic signature that had been established, A-kinase anchor protein 12 (*AKAP12*) was identified as a key mediator underlying oxaliplatin resistance. IL-24 expression was lower, but AKAP12 expression was higher in oxaliplatin-resistant cells (SW480-OxR cells) than in SW480 cells ($p < 0.01$). Expression of AKAP12 in SW480-OxR cells was suppressed by *IL-24* ($p < 0.05$). In SW480-OxR cells, *IL-24* overexpression suppressed proliferation, decreased the JC-1 red/green fluorescence ratio and intracellular ATP levels, and induced apoptosis ($p < 0.05$). Mechanistically, *AKAP12* overexpression reversed the phenotypic changes induced by IL-24, leading to increased resistance to oxaliplatin, enhanced cell growth, and reduced apoptosis ($p < 0.05$).

Conclusion: In colorectal cancer, *IL-24* inhibits tumor progression and reduces oxaliplatin resistance by down-regulating *AKAP12*, highlighting a potentially promising target for therapeutic intervention.

Keywords: colorectal cancer; IL-24; AKAP12; oxaliplatin resistance; prognostic model; mitochondrial function

Introduction

Colorectal cancer (CRC) remains a leading global health concern, with the third-highest incidence and second-highest mortality worldwide [1]. Chemotherapy is still considered the key component of CRC treatment strategy. An oxaliplatin-centered regimen can be used as a first-line treatment for advanced colorectal cancer and can also be used as an auxiliary treatment for patients undergoing surgical resection [2]. The clinical efficacy of oxaliplatin is obviously impaired by drug resistance, and notably, about half of stage II–III CRC patients showed resistance to adjuvant therapy based on oxaliplatin. This drug resistance leads to disease progression and is related to poor prognosis [3]. For these reasons, clarifying the potential mechanisms underlying oxaliplatin resistance and developing novel strategies to overcome this resistance are of great importance.

Copyright: © 2026 The Author(s). Published by Discovery Medicine. This is an open access article under the CC BY 4.0 license.
Note: *Discovery Medicine* stays neutral with regard to jurisdictional claims in published maps and institutional affiliations.

Interleukin-24 (IL-24) is considered a multifunctional cytokine with effective anti-tumor activity [4]. Overexpression of this cytokine inhibits the growth of and induces apoptosis in many cancer cells, but does not exert harmful effects on normal cells [5]. IL-24 not only shows direct anti-tumor properties, but also has the potential to be used as a chemical sensitizer. Previous studies have shown that oxaliplatin resistance in the HT29/oxa CRC cell line may be partially alleviated by IL-24 [6]. Studies have shown that IL-24 can reverse the resistance to cisplatin in lung cancer and regulate the signaling pathways related to chemotherapy resistance in osteosarcoma [7,8]. These findings suggest that IL-24 may be a feasible therapeutic target for overcoming the resistance of platinum drugs. However, the exact mechanism underlying its role in the context of CRC oxaliplatin resistance still needs to be fully elucidated.

Seven oxaliplatin resistance-related genes were found through our bioinformatics research, and a prognostic risk model was established accordingly. After validation in the training and test sets, we focused on A-kinase anchor protein 12 (*AKAP12*). Gene Set Enrichment Analysis (GSEA) showed *AKAP12* may be implicated in the inhibition of mitochondrial protein translation, thus suggesting a potential link between *AKAP12* and mitochondrial function. In the context of CRC, mitochondrial dysfunction is increasingly considered to be related to chemoresistance because of its ability to change the metabolic process, redox balance and apoptosis threshold of cells [9,10]. Therefore, we hypothesized that *AKAP12* may promote the drug resistance of oxaliplatin in CRC through the regulation of mitochondrial function.

The established chemosensitizing function of *IL-24*, combined with our bioinformatics findings linking *AKAP12* to mitochondrial-mediated oxaliplatin resistance, supports our hypothesis that IL-24 may reduce chemotherapy resistance in CRC by down-regulating *AKAP12* and modulating mitochondrial functional parameters. Experimental validation of this *IL-24*/*AKAP12*/mitochondrial function axis (a pathway not previously described) constitutes the primary objective of this study. Such confirmation would not only elucidate a novel mechanism of action of *IL-24* but also indicate the therapeutic potential of targeting this axis.

Materials and Methods

Gene Expression Analysis of IL-24

For an initial exploratory assessment of *IL-24* expression in colorectal cancer-related tissues, data from rectal adenocarcinoma (READ) and colon adenocarcinoma (COAD) were retrieved from the UALCAN database (https://ualcan.path.uab.edu/) and first analyzed. *IL-24* expression was compared between its expression in READ tumor tissues (n = 166) and normal control samples (n = 10), as well as between COAD tumor tissues (n = 286) and normal control samples (n = 41). To assess the association between *IL-24* expression and patient survival, the survival analysis was performed separately for patients with READ and COAD using the UALCAN database.

Assessment of Drug Sensitivity and Functional Enrichment

Using data from the Genomics of Drug Sensitivity in Cancer 2 (GDSC2) database (https://www.cancerrxgene.org/), we investigated the association between *IL-24* expression and oxaliplatin sensitivity in CRC cells.

Identification of IL-24 Pathway-Related Oxaliplatin Resistance Genes

As *IL-24* is known to participate in pathways such as JAK/STAT, SOCS1/3, and p38 MAPK, genes related to these pathways were retrieved. This was accomplished by searching the GeneCards database (https://www.genecards.org/) using the keywords "JAK/STAT pathway", "SOCS1/3 pathway", and "p38 MAPK pathway". Genes with a score greater than 1 were selected, and duplicates were removed, resulting in a final set of 4681 *IL-24* pathway-related genes (**Supplementary Table 1**).

Datasets GSE42387 and GSE76092, which contain mRNA expression profiles from CRC cell lines with acquired oxaliplatin resistance and biological replicates, were obtained from the GEO database. From GSE42387, three oxaliplatin-sensitive and three resistant samples of the HT29 cell line were assigned as the sensitive and resistant groups, respectively. For GSE76092, three untreated HT29 samples and three HTOXAR3 cell line samples were designated as the sensitive and resistant groups. It should be noted that both datasets are based on the HT29 cell line and its oxaliplatin-resistant derivatives. Therefore, the overlapping differentially expressed genes (DEGs) identified across these two datasets represent consistency between datasets derived from the same cellular background rather than true cross-cell-line validation.

Differential gene expression was analyzed dataset-wise via the limma R package (v3.60.3; Parkville, Victoria, Australia). DEGs were defined as those with adjusted $p < 0.05$ and $|\log_2 FC| > 0.585$. The CRC oxaliplatin resistance differential genes were identified by intersecting the up-regulated and down-regulated genes from the resistant groups in both datasets. The overlap between these resistance genes and the *IL-24* pathway-related genes was then determined, yielding the *IL-24* pathway-related oxaliplatin resistance differential genes (ILDEGs, **Supplementary Table 2**). Gene Ontology (GO) and Kyoto Encyclopedia of Genes and Genomes (KEGG) enrichment of the ILDEGs was performed with the clusterProfiler package (v4.12.1, Guangzhou, China) (**Supplementary Table 3**).

Construction and Validation of a Prognostic Signature

To construct a prognostic model, two independent colon cancer transcriptome cohorts, GSE17536 (n = 177) and GSE39582 (n = 573), with complete survival information, were downloaded from the GEO database (https://www.ncbi.nlm.nih.gov/geo/) and designated as the training and validation sets, respectively.

Features were selected from the training set using the Least Absolute Shrinkage and Selection Operator (LASSO) regression algorithm via the glmnet package (v4.1.8; Stanford, CA, USA) in R (R Foundation for Statistical Computing, Vienna, Austria). The optimal penalty parameter (λ) was chosen via 10-fold cross-validation. Based on the LASSO regression results, genes with non-zero coefficients whose signs aligned with the direction of the logFC from the differential expression analysis were selected as the final prognostic signature genes (F-ILDEGs, **Supplementary Table 4**) for CRC patients.

Each patient was assigned a risk score based on the signature, and the median risk score was used as the cutoff to classify them into high-risk and low-risk groups. Signature gene expression in the GSE17536 cohort was visualized using a heatmap (pheatmap; v1.0.12; Tartu, Estonia), and Kaplan-Meier analysis was performed to compare survival between the groups. We employed time-dependent Receiver Operating Characteristic (ROC) curves with the timeROC package (v0.4; Bordeaux, France) to examine how well the risk score predicted outcomes. The GSE39582 cohort confirmed that the risk score is a strong predictor of prognosis.

Functional Enrichment and Drug Sensitivity Based on Risk Groups

Drug sensitivity was analyzed using GDSC2 database-derived data. The relationships between prognostic signature gene expression, the risk score, and oxaliplatin sensitivity were investigated using the oncoPredict package (v1.2; Minneapolis, MN, USA) in R.

DEGs between high- and low-risk groups were identified and ranked by logFC values. GSEA analysis (**Supplementary Table 5**) was conducted on the ranked list via the clusterProfiler package (v4.12.1, Guangzhou, China), with gene set size restricted to 20–1000 genes. The c5.go.v2024.1.Hs.symbols.gmt collection from MSigDB (https://www.gsea-msigdb.org/gsea/msigdb) served as the reference gene set to elucidate pathway differences between the risk groups.

Cell Culture

Human CRC cell line SW480 (CL-0223, Procell, Wuhan, China) and normal colonic epithelial cell line NCM460 (SNL-519, SUNNCELL, Wuhan, China) were cultured in RPMI-1640 complete medium (SNM-001E, SUNNCELL, China) (37 °C, 5% CO_2) in a humidified atmosphere and subcultured every 2–3 days upon reaching 80–90% confluence. The cells were authenticated by short tandem repeat (STR) profiling and tested negative for mycoplasma contamination.

The oxaliplatin-resistant SW480-OxR cell line was generated through stepwise adaptation of the parental SW480 cells to escalating doses of oxaliplatin (HY-17371, MedChemExpress, Shanghai, China) as previously described [11]. Cells underwent 0.5 μM oxaliplatin treatment; after 2 weeks of stable growth, the drug concentration was gradually increased (0.5→1→2→4→6 μM) every 2 weeks. Resistant cells (SW480-OxR) were maintained in medium containing 4 μM oxaliplatin and cultured in drug-free medium for 2 weeks before further analyses.

Recombinant Adenovirus and Plasmid Transfection

Recombinant adenoviruses encoding human *IL-24* (Ad.IL-24) and empty control adenovirus (Ad.vector) were constructed and packaged by Hanbio (Shanghai, China). For *IL-24* overexpression, SW480 or SW480-OxR cells in 6-well plates (2×10^5/well) were incubated for 24 h, then transduced with Ad.IL-24 or Ad.vector at a multiplicity of infection (MOI) of 50 for 48 h.

For *AKAP12* overexpression, the complete coding sequence of human *AKAP12* (**Supplementary Material**) was inserted into the pcDNA3.1(+) vector (VT1001, YouBio, Changsha, China), with empty pcDNA3.1(+) as the negative control (NC). SW480-OxR cells in 6-well plates (2×10^5/well) were transfected with pcDNA3.1-AKAP12 or NC using Lipo8000™ transfection reagent (C0533, Beyotime, Shanghai, China). Overexpression efficiency was verified by quantitative real-time polymerase chain reaction (qRT-PCR) 48 h post-transfection.

Cell Viability

Cell viability was determined by the cell counting kit-8 (CCK-8) assay (A311-01, Vazyme, Nanjing, China). Cells in 96-well plates (5×10^3/well) were cultivated for 24 h, followed by treatment (e.g., adenovirus transduction, drug exposure) as indicated. At the specified time points, 10 μL CCK-8 reagent was added to each well, followed by a 2-h incubation (37 °C). Cell viability was measured by a microplate reader (iMark™, Bio-Rad, Hercules, CA, USA) at 450 nm absorbance.

Clonogenic Assay

Cells (500/well) in a 6-well plate were cultured for 10–14 days. The culture medium was updated every three days. Once colonies formed, they were fixed (4% paraformaldehyde; T19998, Saint-Bio, Shanghai, China), stained (0.1% crystal violet; R23711, Saint-Bio, Shanghai, China) for 20 min, and then washed (phosphate-buffered saline (PBS); T21925, Saint-Bio, Shanghai, China).

Cell Apoptosis

Cells were collected, washed twice with ice-cold PBS and resuspended in Annexin V Binding Buffer. Cells (1×10^6/mL) were analyzed for apoptosis with annexin V-fluorescein isothiocyanate (FITC)/propidium iodide (PI) double staining kit (PH0539, PHYGENE, Fuzhou, China). A 100 µL aliquot of cell suspension was dyed (5 µL Annexin V-FITC and 5 µL PI), incubated (15 min, room temperature, in the dark), and analyzed on a BD FACSCanto II flow cytometer (BD Biosciences, San Jose, CA, USA), and the resulting data were analyzed with FlowJo software (v10.8, BD Biosciences, Franklin Lakes, NJ, USA).

qRT-PCR

Total RNA was purified from cells using a commercial RNA extraction kit (AG21023, Agbio, Hunan, China). cDNA was synthesized from 1 µg of RNA with a reverse transcription kit (A232, GenStar, Beijing, China). Quantitative PCR was performed using SYBR Green master mix (A301, GenStar, China) on a QuantStudio 6 Flex Real-Time PCR System (Applied Biosystems, Foster City, CA, USA). Each sample was assayed in triplicate, with expression normalized to glyceraldehyde-3-phosphate dehydrogenase (GAPDH) and calculated by the $2^{-\Delta\Delta CT}$ method. Primers are provided in Table 1.

Table 1. Primers used in this study.

Genes (human)	5′--> 3′
IL-24 F	AGGACCAGAGGGACAAGACAT
IL-24 R	GCAGGGTGTGGACAAGGTAA
AKAP12 F	AAGCAAATGGGGACTCGGAC
AKAP12 R	AGCCTGCGAATGAAGGAGAC
GAPDH F	GTCTCCTCTGACTTCAACAGCG
GAPDH R	ACCACCCTGTTGCTGTAGCCAA

Abbreviation: F, Forward; R, Reverse; *IL-24*, interleukin-24; *AKAP12*, A-kinase anchor protein 12; *GAPDH*, glyceraldehyde-3-phosphate dehydrogenase.

Western Blotting

Cells were lysed in RIPA buffer (AP01L013, LifeiLab, Shanghai, China), and protein concentrations were determined with a BCA assay kit (YWB002, YFXBIO, Nanjing, China). Equal amounts of protein were resolved by SDS-PAGE (190916-40, YaJi Biological, Shanghai, China), transferred onto PVDF membranes (0WJ001S, Epizyme, Shanghai, China), blocked (AP36L118, LifeiLab, Shanghai, China), and probed with primary antibodies (Table 2) (overnight, 4 °C). After thorough washing, the blots were incubated with appropriate HRP-conjugated secondary antibodies (Table 2). Protein bands were detected using an ECL substrate (YWB003, YFXBIO, Nanjing, China), and images were acquired using a SynGene G:BOX F3 system (Syngene, Cambridge, UK).

Table 2. Antibodies used in this study.

Name	Catalog	Dilution	Manufacturer
IL-24	DF6672	1/1000	Affinity, USA
AKAP12	DF8813	1/1000	Affinity, USA
GAPDH	ab8245	1/10,000	Abcam, UK
Goat anti-rabbit	ab205718	1/2000	Abcam, UK
Goat anti-mouse	ab205719	1/2000	Abcam, UK

Mitochondrial Membrane Potential (MMP) Detection

The JC-1 assay kit (40705ES03, YEASEN, Shanghai, China) was used to analyze MMP. After treatment, cells were washed with PBS and stained with a 10 µM JC-1 working solution (20 min, 37 °C). Following two washes in the supplied staining buffer, fluorescence imaging was carried out using a fluorescence microscope (Olympus IX73; Olympus, Tokyo, Japan). Red fluorescence from JC-1 aggregates shows normal MMP, while green fluorescence from monomers shows mitochondrial depolarization. The red/green (aggregate/monomer) fluorescence intensity ratio was quantified using ImageJ software (version 1.52, NIH, Bethesda, MD, USA) to assess MMP changes, and a decreased red/green ratio indicating mitochondrial depolarization and a reduced MMP.

ATP Content Assay

Intracellular ATP content was quantified using a commercial assay kit (Beyotime, China, S0026). After treatment, cells were collected and lysed. The resulting lysate was centrifuged (12,000 ×g, 4 °C, 5 min; Eppendorf 5424 R, Eppendorf, Hamburg, Germany), and the supernatant was mixed with the ATP detection working solution, and luminescence was measured using a microplate reader. Relative ATP levels were calculated based on a standard curve generated from continuously diluted ATP standard solution.

Statistical Analysis

At least three independent replicates were performed for each experiment. Data were analyzed with the SPSS 21.0 software package (SPSS Inc., Chicago, IL, USA) and presented as the mean ± standard deviation. Data normality was assessed by Shapiro-Wilk testing, and homogeneity of variance was assessed by Levene's test. For comparisons among multiple groups, one-way or two-way analysis of variance (ANOVA) was employed, followed by Tukey's post-hoc test. Statistical significance was set at $p < 0.05$.

Results

Clinical and Cellular Expression Patterns of IL-24 in CRC

As an initial exploratory observation, *IL-24* expression in tumor tissues from READ and COAD patients was significantly increased compared with normal tissues in the UALCAN database (Fig. 1A,B, $p < 0.001$). In survival

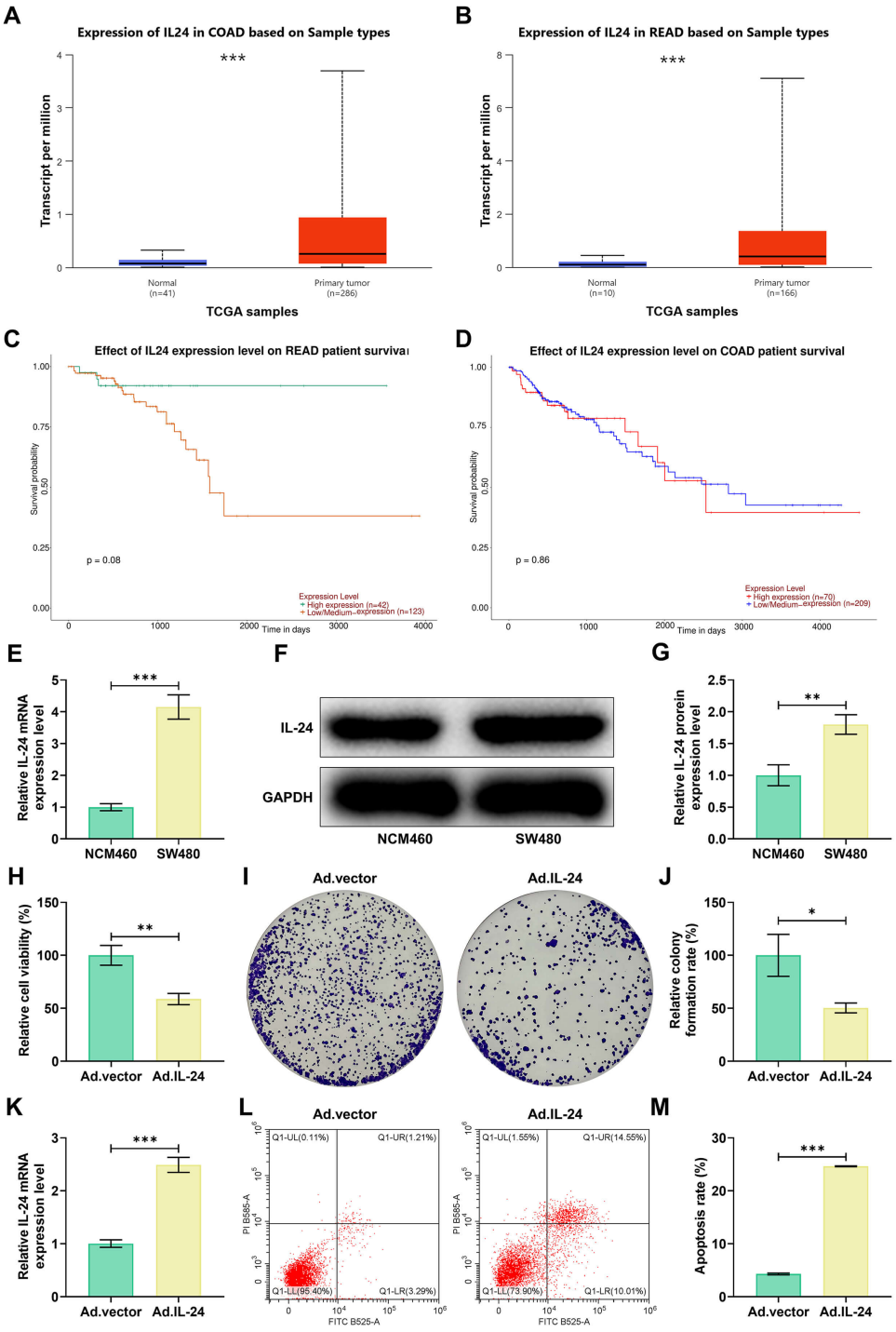


Fig. 1. IL-24 is upregulated in rectal adenocarcinoma and inhibits CRC progression via inducing apoptosis. (A,B) *IL-24* levels in human rectal adenocarcinoma (READ) tissues (n = 166) and normal tissues (n = 10), and its level in human colon adenocarcinoma (COAD) tumor tissues (n = 286) and normal control samples (n = 41). (C,D) Kaplan-Meier overall survival curves of READ or COAD patients. (E) *IL-24* mRNA levels in normal colonic epithelial cell line (NCM460) and colorectal cancer cell line (SW480) (qRT-PCR). (F,G) IL-24 protein expression in NCM460 and SW480 cells (Western blotting). (H) Viability of SW480 cells transfected with empty adenoviral vector (Ad.vector) or IL-24-overexpressing adenovirus (Ad.IL-24) (CCK-8 assay). (I,J) Representative images and quantitative analysis of colony formation assay for SW480 cells treated with Ad.vector or Ad.IL-24. (K) *IL-24* mRNA levels in SW480 cells transfected with empty adenoviral vector (Ad.vector) or IL-24-overexpressing adenovirus (Ad.IL-24) (qRT-PCR). (L,M) Apoptosis of SW480 cells treated with Ad.vector or Ad.IL-24 (flow cytometry). Data are expressed as mean ± standard deviation (SD) (n = 3). $^{*}p < 0.05$, $^{**}p < 0.01$, $^{***}p < 0.001$. CRC, colorectal cancer; qRT-PCR, quantitative real-time polymerase chain reaction.

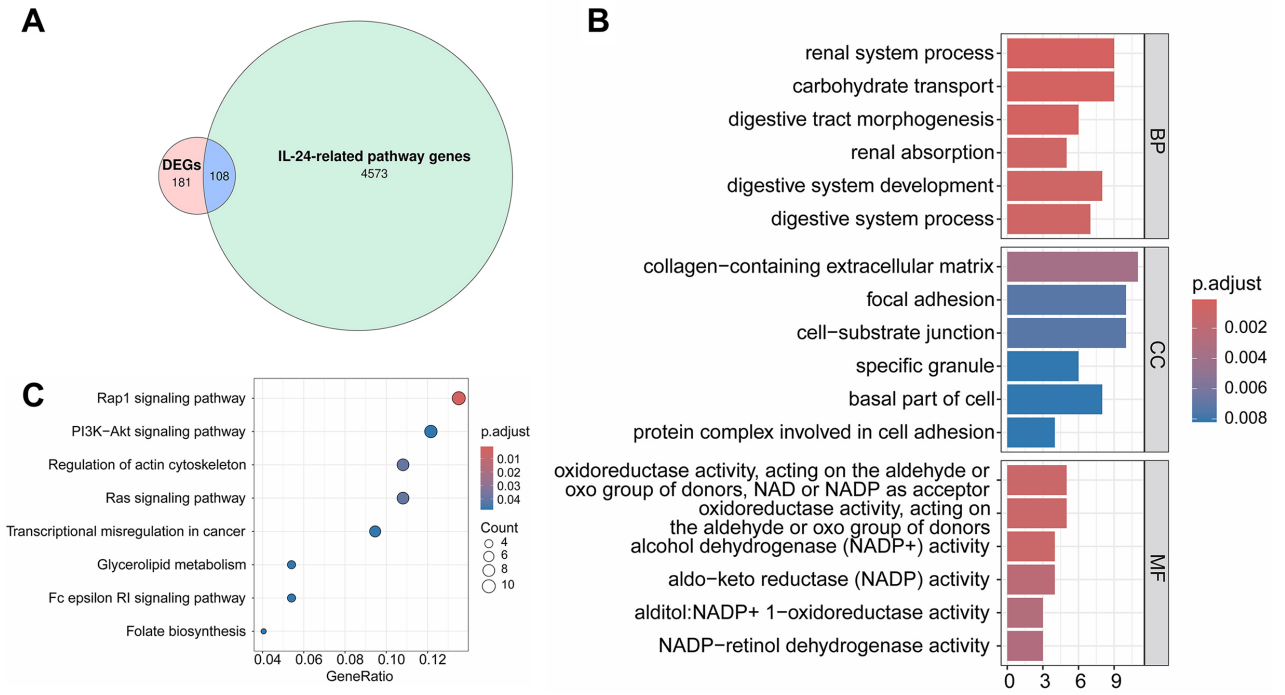


Fig. 2. Identification of IL-24-associated DEGs and their functional enrichment in CRC. (A) Venn diagram displaying the intersection between *IL-24*-related pathway genes and the combined DEGs (from GSE42387 and GSE76092). (B) Bar plot of Gene Ontology (GO) functional enrichment. (C) Bubble plot of Kyoto Encyclopedia of Genes and Genomes (KEGG) pathway enrichment. DEGs, differentially expressed genes.

analysis, low *IL-24* expression was associated with a poorer survival trend in READ patients, but the difference is not statistically significant (Fig. 1C, $p = 0.08$); no significant association was observed in COAD patients ($p = 0.86$, Fig. 1D). We also observed that *IL-24* mRNA and protein levels were up-regulated in SW480 CRC cells compared with NCM460 normal colon epithelial cells (Fig. 1E–G, $p < 0.01$). *IL-24* overexpression in SW480 cells significantly reduced cell viability (Fig. 1H, $p < 0.01$). The elevated *IL-24* expression in SW480 cells was confirmed by qRT-PCR (Fig. 1K, $p < 0.001$). Moreover, *IL-24* overexpression impaired colony formation (Fig. 1I,J, $p < 0.05$) and triggered a marked increase in apoptosis (Fig. 1L,M, $p < 0.001$), collectively indicating its growth-inhibitory function.

Identification of IL-24-Associated DEGs and Their Functional Enrichment Profiles

The upregulated and downregulated genes of CRC transcriptome datasets GSE42387 and GSE76092 were intersected, and a total of 289 intersecting DEGs were selected from the two datasets, including 120 up-regulated genes and 169 down-regulated genes (**Supplementary Fig. 1A–D**). These 289 up/down-regulated genes intersect with *IL-24* signal-related genes to obtain 108 genes (Fig. 2A). Functional enrichment analysis of these 108 genes revealed their involvement in digestive system development and biological processes related to extracellular matrix tissue (Fig. 2B). These genes were obviously enriched in cancer-related signaling pathways, particularly the Rap1 and PI3K-Akt pathways (Fig. 2C).

Development and Validation of a Prognostic Model Based on F-ILDEGs

Firstly, the LASSO regression with 10-fold cross-validation was applied to the GSE17536 training cohort, and the features were refined into seven key F-ILDEGs (Fig. 3A,B). Risk scores were computed for each patient based on the selected features, and the median risk score served as the cutoff to classify patients into high-risk and low-risk groups (Fig. 3C,D). Examination of gene expression in these populations showed that *AKAP12* and *FGFBP1* were upregulated, while *UGDH*, *MVP*, *INPP5D*, *FGFR3* and *HNF1A* were downregulated in high-risk patients (Fig. 3E). We evaluated the prognostic performance of the risk score in the training set and found that the training set effectively predicted the overall survival (OS) of 1, 3, 5 and 10 years, yielding area under the receiver operating characteristic curve (AUC) values of 0.83, 0.79, 0.82 and 0.82 (Fig. 3F). Consistently, the high-risk group exhibited poorer OS than the low-risk group, as revealed by Kaplan-Meier survival analysis (Fig. 3G). Of note, although this risk model is derived from *IL-24* pathway-related genes, the high-risk group does not directly represent *IL-24* high expression; rather, it captures a transcriptional state asso-

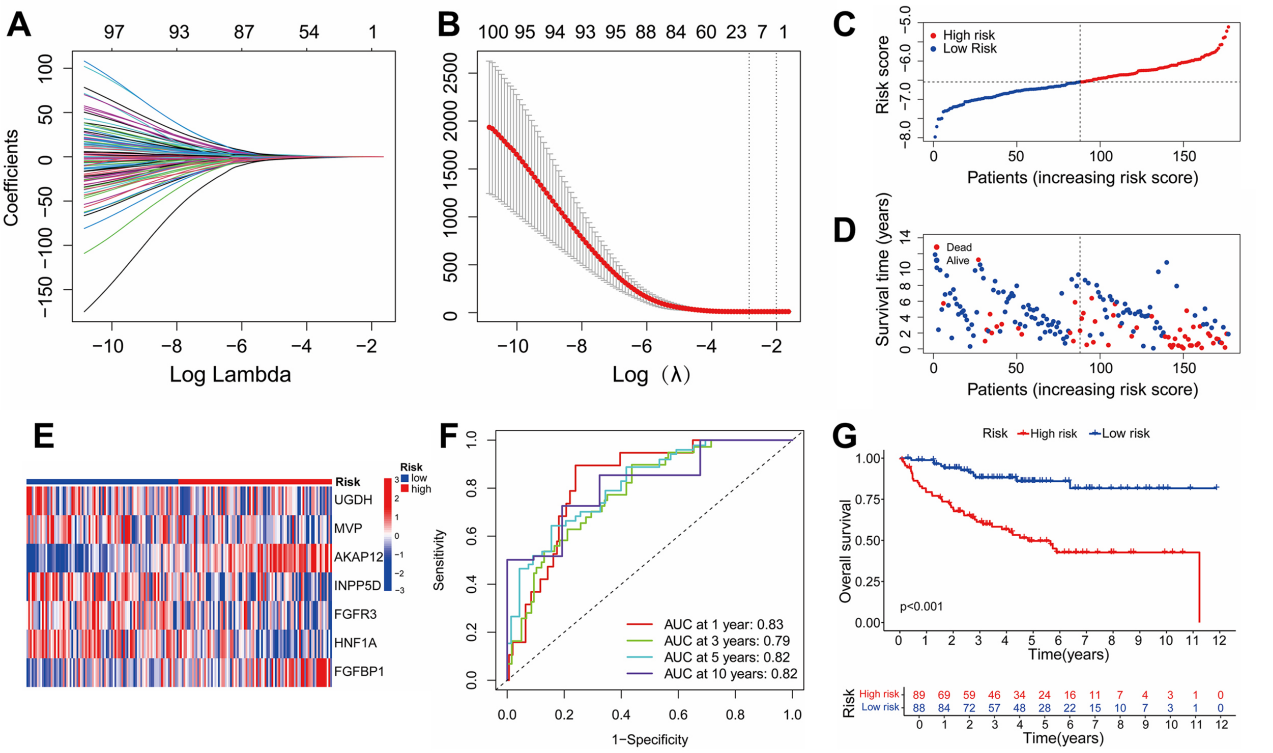


Fig. 3. Development and prognostic evaluation of a signature via LASSO regression. (A) Coefficient profile plot of genes in LASSO regression. (B) 10-fold cross-validation plot for optimal Lambda (λ) selection in LASSO regression. (C) Risk score distribution of CRC patients in the training cohort, stratified into high-risk (red) and low-risk (blue) groups based on the median risk score. (D) Survival status and survival time of patients in the training cohort, corresponding to the risk score order in (C). (E) Based on the LASSO regression analysis results, genes with regression coefficient signs consistent with the direction of logFC in DEGs were selected as prognostic signature genes for CRC patients, totaling seven genes. (F) ROC curves of the risk score model in the training cohort. (G) Kaplan-Meier (KM) survival curve comparing overall survival between high-risk and low-risk groups in the training cohort. LASSO, Least Absolute Shrinkage and Selection Operator; ROC, Receiver Operating Characteristic.

ciated with *IL-24* downstream dysregulation. The analysis of a single gene linked the high expression of *AKAP12* and *FGFBP1* with poorer OS (**Supplementary Fig. 1E,F**), whereas the low expression of *HNF1A* and *INPP5D* was associated with a lower survival rate (**Supplementary Fig. 1G,H**).

We used an independent validation dataset to evaluate the model. Based on the risk score distribution of F-ILDEGs and the status of CRC patients, it can be seen that patients in the high-risk group had shorter survival (**Supplementary Fig. 2A,B**). The expression differences of the seven genes in the high- and low-risk groups in the validation dataset were consistent with those observed in the training set (**Supplementary Fig. 2C**). In the validation set, patients in the high-risk group had significantly shorter survival compared to those in the low-risk group ($p = 0.034$) (**Supplementary Fig. 2D**). In addition, patients in the *AKAP12* high-expression group had significantly shortened survival in the validation set ($p = 0.023$, **Supplementary Fig. 2E**). Interestingly, the *FGFR3*-OS association was significant in the validation cohort ($p = 0.017$, **Supplementary Fig. 2F**).

Drug Sensitivity Analysis and Functional Exploration of AKAP12

Then we evaluated the sensitivity of oxaliplatin using the GDSC2 database and the oncoPredict algorithm. First, the high-risk group showed greater drug resistance than the low-risk group (**Supplementary Fig. 2G**). High expression of *AKAP12* and *FGFBP1* showed higher resistance than their low-expression groups (**Supplementary Fig. 2H,I**), while the low expression of *HNF1A* showed higher resistance than its high expression (**Supplementary Fig. 2J**). In view of the consistency of *AKAP12* expression results in all data sets, *AKAP12* was selected for GSEA analysis. As shown in Fig. 4A, *AKAP12* was positively associated with ECM organization-related pathways (Fig. 4A). At the same time, *AKAP12* was negatively associated with pathways related to core cell functions, such as mitochondrial translation and inhibition of DNA replication (replicon) (Fig. 4B).

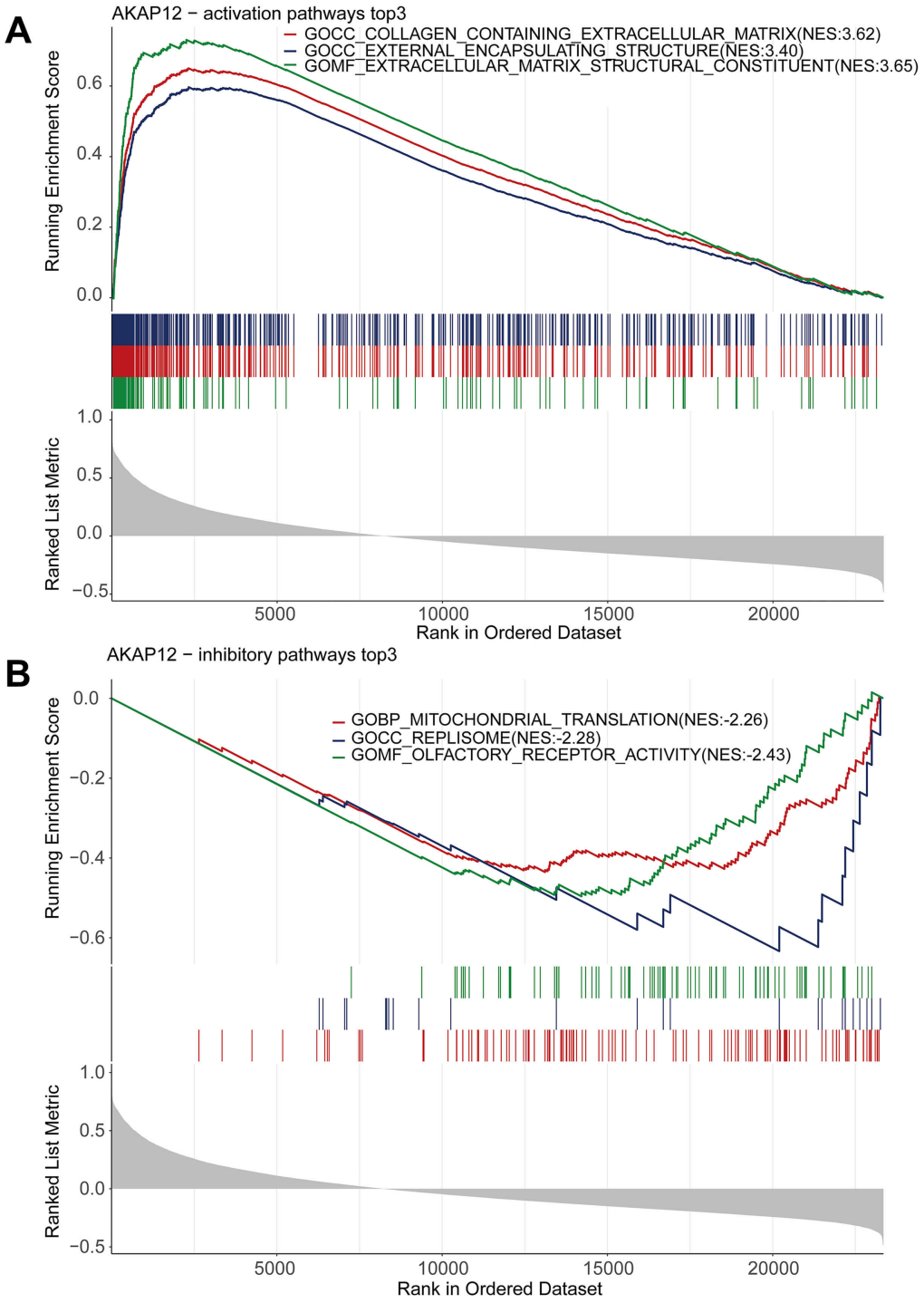


Fig. 4. GSEA analysis of AKAP12-associated signaling pathways. (A) GSEA results for pathways positively associated with *AKAP12* expression. (B) GSEA results for pathways negatively associated with *AKAP12* expression. GSEA, Gene Set Enrichment Analysis.

IL-24 Negatively Regulates AKAP12 in an Oxaliplatin-Resistance Model

Oxaliplatin-resistant SW480-OxR cells showed a significantly higher survival rate than SW480 cells when treated with OXA at concentrations ranging from 5 to 40 μM (Fig. 5A, $p < 0.001$). In these drug-resistant cells, we found that *IL-24* was significantly downregulated and AKAP12 was significantly upregulated (Fig. 5B–F, $p < 0.01$). Adenovirus-mediated *IL-24* overexpression (Ad.IL-24) significantly downregulated AKAP12 (Fig. 5G–I, $p < 0.05$). These results confirmed *IL-24* as a negative regulator of *AKAP12*.

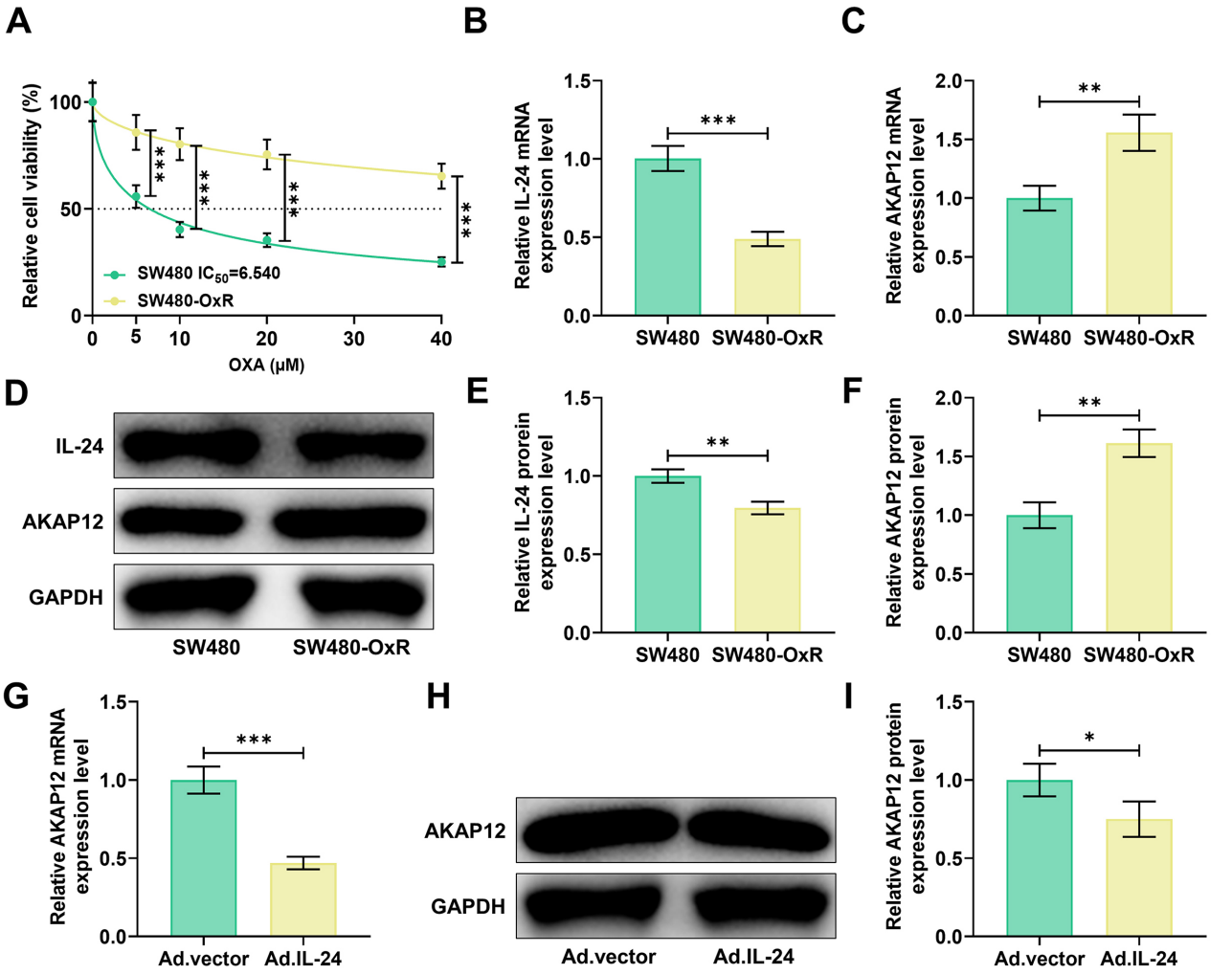


Fig. 5. IL-24 and AKAP12 expression in oxaliplatin-resistant SW480-OxR cells and IL-24-mediated regulation of AKAP12. (A) Viability of parental SW480 cells and oxaliplatin-resistant SW480-OxR cells treated with increasing concentrations of oxaliplatin (OXA) (CCK-8). (B,C) *IL-24* (B) and *AKAP12* (C) mRNA levels in SW480 and SW480-OxR cells (Quantitative analysis). (D–F) IL-24 and AKAP12 protein expression in SW480 and SW480-OxR cells (Western blotting). (G) *AKAP12* mRNA expression in SW480-OxR cells transfected with an empty adenoviral vector (Ad.vector) or *IL-24*-overexpressing adenovirus (Ad.IL-24) (qRT-PCR analysis). (H,I) AKAP12 protein expression in Ad.vector- or Ad.IL-24-transfected SW480-OxR cells (Western blotting). Data are expressed as mean ± SD (n = 3). $^{*}p < 0.05$, $^{**}p < 0.01$, $^{***}p < 0.001$.

AKAP12 Overexpression Counteracts IL-24-Mediated Effects in SW480-OxR Cells

After confirming the successful overexpression of *AKAP12* (Fig. 6A, $p < 0.01$), we evaluated the influence of the *IL-24*/*AKAP12* axis on the malignant biological behavior of cells. Ad.IL-24 reversed oxaliplatin resistance (Fig. 6B, $p < 0.05$), inhibited colony formation (Fig. 6C,F, $p < 0.05$), and induced apoptosis (Fig. 6D,G, $p < 0.001$). Ad.IL-24 treatment also regulated multiple mitochondrial functional parameters: it decreased the JC-1 aggregate/-monomer ratio (Fig. 6E,H, $p < 0.01$) and ATP level (Fig. 6I, $p < 0.05$). Crucially, *AKAP12* overexpression increased the JC-1 aggregate/monomer ratio and ATP level (Fig. 6E,H,I, $p < 0.05$), and it also reversed the above-mentioned effects of Ad.IL-24 (Fig. 6B–I, $p < 0.05$). These results indicate that *AKAP12* is a key functional downstream mediator of IL-24, through which IL-24 regulates chemical sensitivity and cell phenotype.

Discussion

The antitumor activity of *IL-24* in CRC has been fully proven [12,13]. Our findings corroborate and extend these observations. Of note, *IL-24* expression was elevated in READ tumor tissues and SW480 cells compared with their respective normal controls, and *IL-24* overexpression suppressed malignant phenotypes. This apparent discrepancy may be explained by the fact that tissue-level *IL-24* reflects the contribution of multiple cell types, including immune

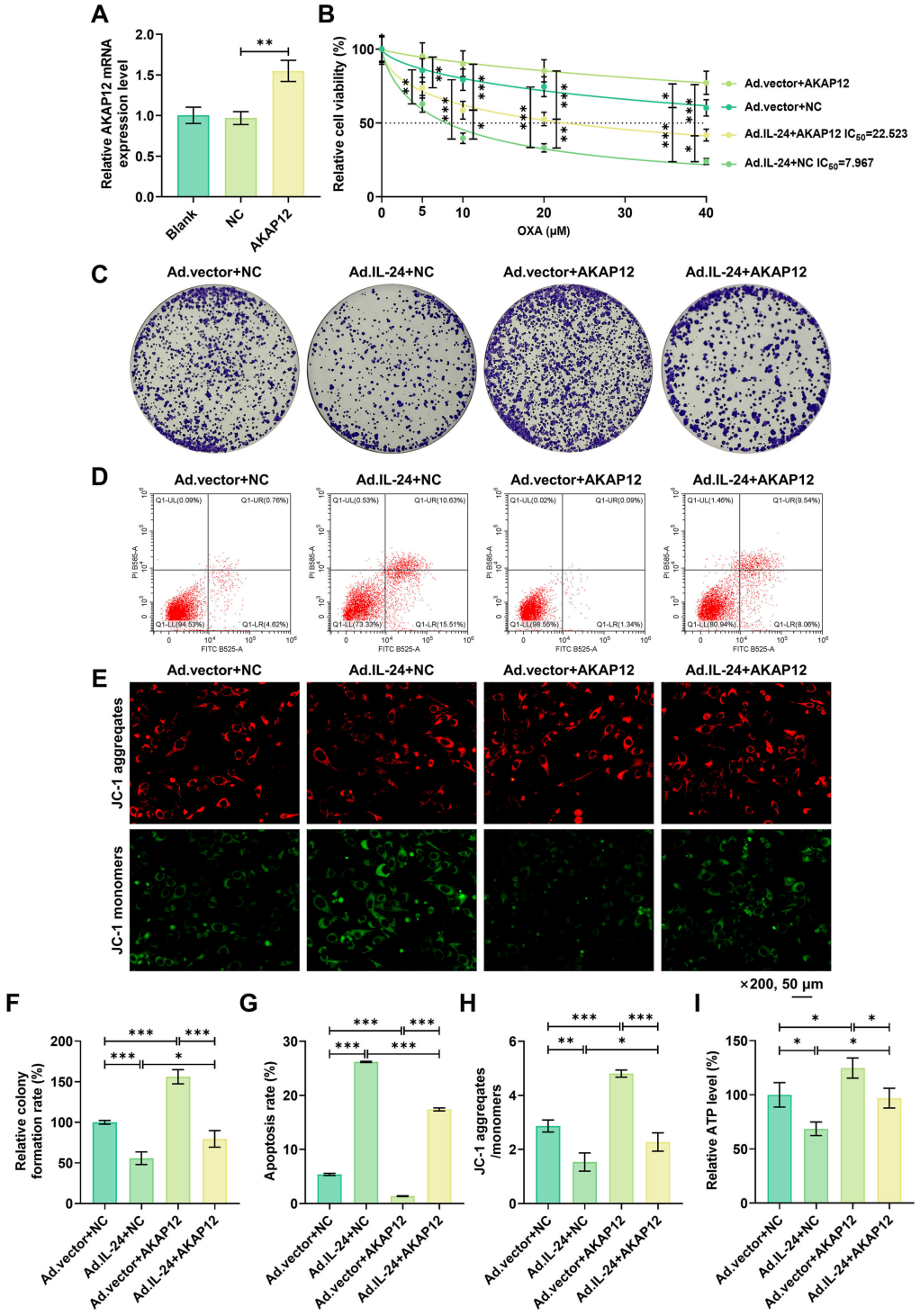


Fig. 6. The *IL-24-AKAP12* pathway modulates mitochondrial function parameters to sensitize CRC cells to oxaliplatin. (A) *AKAP12* mRNA expression in SW480-OxR cells transfected with negative control (NC), or *AKAP12* overexpression vector (qRT-PCR analysis). (B) Viability of SW480-OxR cells (CCK-8). (C,F) Representative images (C) and quantitative analysis (F) of colony formation in SW480-OxR cells under oxaliplatin treatment (10 μM, 48 h) (colony formation assay). (D,G) Representative flow cytometry plots (D) and quantitative analysis (G) of apoptosis in SW480-OxR cells under oxaliplatin treatment (10 μM, 48 h) (flow cytometry). (E,H) Representative images (E) and quantitative analysis (H) of JC-1 fluorescence staining in SW480-OxR cells under oxaliplatin treatment (10 μM, 48 h). The JC-1 red/green (aggregate/monomer) fluorescence ratio was used to indicate MMP; a higher ratio reflects a higher MMP. Scale bar = 50 μm. 200×. (I) Adenosine triphosphate (ATP) levels in SW480-OxR cells under oxaliplatin treatment (10 μM, 48 h). Data are expressed as mean ± SD (n = 3). $^{*}p < 0.05$, $^{**}p < 0.01$, $^{***}p < 0.001$.

and stromal cells, whereas cell-line data reflect tumor-cell-intrinsic expression. Elevated *IL-24* in tumor tissue may therefore represent a compensatory or inflammatory response, while low *IL-24* may reflect impaired downstream tumor-suppressive signaling or weakened immune surveillance. Accordingly, endogenous *IL-24* expression and exogenous *IL-24*-mediated therapeutic effects should be interpreted as related but not equivalent biological processes. The prognostic model we constructed showed good performance in predicting the OS in the training and independent verification sets. Specifically, the predicted AUC of OS in the training set for 1/3/5/10 years reached 0.83, 0.79, 0.82 and 0.82, respectively. These results show that the prediction performance is comparable to or may even be better than the previously published prognostic model for CRC [14,15].

The analysis defined a high-risk transcriptional pattern, characterized by increased *AKAP12* and *FGFBP1* and decreased expression of five other genes (*UGDH*, *MVP*, *INPP5D*, *FGFR3*, *HNF1A*). A significant correlation was observed between this pattern and prognostic trends in the CRC cohort. The role of FGFBP1, a fibroblast growth factor binding protein reported to promote tumor angiogenesis and invasion through interaction with FGFs, is supported by its known high expression in CRC and facilitation of metastasis [16]. Additionally, FGFBP1 has been reported to participate in bevacizumab resistance in CRC by inducing FAPα expression [17]. The present study has further revealed an association between high *FGFBP1* expression and oxaliplatin resistance, thereby extending the known role of *FGFBP1* in chemotherapy resistance. *HNF1A* belongs to the hepatocyte nuclear factor family and has been linked to cancer growth and resistance to oxaliplatin [18]. Consistent with previous findings, we observed that low *HNF1A* expression was linked to poor prognosis and resistance to oxaliplatin. *INPP5D*, a phosphatidylinositol phosphatase that inhibits the PI3K/Akt pathway [19], functions as a tumor suppressor. Reduced *INPP5D* expression has been associated with adverse clinical outcomes, consistent with the established oncogenic role of PI3K/Akt signaling in CRC [20]. While mutations of the receptor tyrosine kinase *FGFR3* have been reported in CRC [21,22], its prognostic relevance remains debated. In this study, its prognostic impact was found to be significant only within the validation cohort, a discrepancy potentially attributable to genetic heterogeneity and warranting further investigation with larger sample sizes.

AKAP12 plays a central role in oxaliplatin resistance. Specifically, *AKAP12* is significantly up-regulated in oxaliplatin-resistant SW480-OxR cells, and *IL-24* reduces drug resistance by down-regulating *AKAP12*. Although previous studies have shown that the deletion of *AKAP12* inhibits the proliferation and stem cell characteristics of CRC cells [23], our results show that its overexpression promotes the malignant phenotype in chemotherapy-resistant cells. GSEA analysis showed that *AKAP12* regulated mitochondrial translation and the replicon pathway. Subsequent functional assays confirmed that *AKAP12* overexpression increased MMP and ATP production. Furthermore, our results revealed that *IL-24* can regulate mitochondrial function and membrane integrity through the suppression of *AKAP12*. Although *IL-24* can induce cancer cell apoptosis by affecting mitochondrial function and ROS production [24], whether *IL-24* participates in chemotherapy resistance through this regulatory mechanism remains unknown. It is worth noting that mitochondrial dysfunction is considered one of the reasons for oxaliplatin resistance [25]: impaired mitochondrial function can promote drug resistance by reducing ROS production and enhancing DNA damage repair [26]. Moreover, it has been confirmed that oxaliplatin resistance in CRC can be reversed through mitochondrial-targeted nano-drugs that induce mitochondrial dysfunction and apoptosis [27]. Therefore, our findings suggest that AKAP12 may contribute to oxaliplatin resistance by modulating mitochondrial function in resistant CRC cells.

There are some limitations in this study that need to be acknowledged. First, the oxaliplatin-resistant cell model was established exclusively in the SW480 cell line, and all functional validation experiments were performed in this single cellular background. Given the heterogeneity of CRC and its diverse molecular subtypes, the findings derived from a single cell line may not fully represent the entire spectrum of CRC, and the generalizability of our conclusions to other CRC cell lines remains to be established. Second, bioinformatics analysis relies on public datasets and lacks independent validation using clinical samples. Third, *AKAP12* overexpression in rescue experiments was verified only at the mRNA level by qRT-PCR, whereas protein-level validation by Western blot was not performed. Fourth, the specific molecular mechanism of IL-24's negative regulation of *AKAP12* has not been clarified, and whether this regulatory effect is direct or indirect remains to be analyzed. Finally, the study has not been verified *in vivo* by an animal model to evaluate the effect of the *IL-24*/*AKAP12* axis on tumor growth and drug resistance, and its physiological correlation is still uncertain.

Conclusion

To sum up, the 7-gene prognostic model based on *IL-24*-related genes shows a robust predictive efficiency, among which *FGFBP1*, *HNF1A* and other genes can be used as potential prognostic biomarkers. At the mechanistic level, the study provides evidence that *IL-24* can reverse oxaliplatin resistance by downregulating *AKAP12* and regulating mitochondrial function parameters, which provides a new molecular target for prognosis evaluation of CRC and reversing oxaliplatin resistance. Future research needs to expand the verification scope of cell lines and clinical samples, clarify the specific mechanisms of *IL-24* regulating *AKAP12*, and verify the efficacy of targeting this pathway

through animal experiments, thus paving the way for novel precision treatment strategies for CRC.

Availability of Data and Materials

The datasets used or analyzed during the current study are available from the corresponding authors upon reasonable request.

Author Contributions

ZJF, YYH and WSL designed the research study; ZJF, YYH, MJZ and WSL performed the research; MJZ, HMM and CJG collected and analyzed the data. ZJF and WSL have been involved in drafting the manuscript and all authors have been involved in revising it critically for important intellectual content. All authors gave final approval of the version to be published. All authors have participated sufficiently in the work to take public responsibility for appropriate portions of the content and agreed to be accountable for all aspects of the work in ensuring that questions related to its accuracy or integrity.

Ethics Approval and Consent to Participate

Not applicable.

Acknowledgment

Not applicable.

Funding

This work was supported by the National Natural Science Foundation of China [grant number: 82303594], Zhejiang Medical and Health Science and Technology Plan [grant number: 2024XY091], and Zhejiang Provincial County Level Advantageous Disciplines of Traditional Chinese Medicine Construction Plan [grant number: 2023-XK-D040].

Conflict of Interest

The authors declare no conflict of interest.

Supplementary Material

Supplementary material associated with this article can be found, in the online version, at https://doi.org/10.24976/Discov.Med.202638214.285.

References

[1] Klimeck L, Heisser T, Hoffmeister M, Brenner H. Colorectal cancer: A health and economic problem. Best Practice & Research. Clinical Gastroenterology. 2023; 66: 101839. https://doi.org/10.1016/j.bpg.2023.101839

[2] Adebayo AS, Agbaje K, Adesina SK, Olajubutu O. Colorectal Cancer: Disease Process, Current Treatment Options, and Future Perspectives. Pharmaceutics. 2023; 15: 2620. https://doi.org/10.3390/pharmaceutics15112620

[3] Zeng K, Li W, Wang Y, Zhang Z, Zhang L, Zhang W, et al. Inhibition of CDK1 Overcomes Oxaliplatin Resistance by Regulating ACSL4-mediated Ferroptosis in Colorectal Cancer. Advanced Science (Weinheim, Baden-Wurttemberg, Germany). 2023; 10: e2301088. https://doi.org/10.1002/advs.202301088

[4] Modi J, Roy A, Pradhan AK, Kumar A, Talukdar S, Bhoopathi P, et al. Insights into the Mechanisms of Action of MDA-7/IL-24: A Ubiquitous Cancer-Suppressing Protein. International Journal of Molecular Sciences. 2021; 23: 72. https://doi.org/10.3390/ijms23010072

[5] Raguraman R, Munshi A, Ramesh R. Interleukin-24: A Multidimensional Therapeutic for Treatment of Human Diseases. Wiley Interdisciplinary Reviews. Nanomedicine and Nanobiotechnology. 2025; 17: e70013. https://doi.org/10.1002/wnan.70013

[6] Chang S, Yang J, Chen W, Xie Y, Sheng W. Antitumor activity of an adenovirus harboring human IL-24 in colon cancer. Molecular Biology Reports. 2011; 38: 395–401. https://doi.org/10.1007/s11033-010-0121-3

[7] Zhang L, Wang Y, Li X, Xia X, Li N, He R, et al. ZBTB7A Enhances Osteosarcoma Chemoresistance by Transcriptionally Repressing lncRNALINC00473-IL24 Activity. Neoplasia. 2017; 19: 908–918. https://doi.org/10.1016/j.neo.2017.08.008

[8] Xu M, Tang X, Guo J, Sun W, Tang F. Reversal effect of adenovirus-mediated human interleukin 24 transfection on the cisplatin resistance of A549/DDP lung cancer cells. Oncology Reports. 2017; 38: 2843–2851. https://doi.org/10.3892/or.2017.6002

[9] Wang B, Guo X, Qin L, He L, Li J, Jin X, et al. Pharmacological modulation of mitochondrial function as novel strategies for treating intestinal inflammatory diseases and colorectal cancer. Journal of Pharmaceutical Analysis. 2025; 15: 101074. https://doi.org/10.1016/j.jpha.2024.101074

[10] Mani S, Ralph SJ, Swargiary G, Rani M, Wasnik S, Singh SP, et al. Therapeutic Targeting of Mitochondrial Plasticity and Redox Control to Overcome Cancer Chemoresistance. Antioxidants & Redox Signaling. 2023; 39: 591–619. https://doi.org/10.1089/ars.2023.0379

[11] Sun W, Li J, Zhou L, Han J, Liu R, Zhang H, et al. The c-Myc/miR-27b-3p/ATG10 regulatory axis regulates chemoresistance in colorectal cancer. Theranostics. 2020; 10: 1981–1996. https://doi.org/10.7150/thno.37621

[12] Lu Y, Yu Y, Liu F, Han Y, Xue H, Sun X, et al. LINC00511-dependent inhibition of IL-24 contributes to the oncogenic role of HNF4α in colorectal cancer. American Journal of Physiology. Gastrointestinal and Liver Physiology. 2021; 320: G338–G350. https://doi.org/10.1152/ajpgi.00243.2020

[13] Smith S, Lopez S, Kim A, Kasteri J, Olumuyide E, Punu K, et al. Interleukin 24: Signal Transduction Pathways. Cancers. 2023; 15: 3365. https://doi.org/10.3390/cancers15133365

[14] Hong J, Lin X, Hu X, Wu X, Fang W. A Five-gene Signature for Predicting the Prognosis of Colorectal Cancer. Current Gene Therapy. 2021; 21: 280–289. https://doi.org/10.2174/1566523220666201012151803

[15] Zhao T, Zhang X, Liu X, Jiang X, Chen S, Li H, et al. Characterizing PANoptosis gene signature in prognosis and chemosensitivity of colorectal cancer. Journal of Gastrointestinal Oncology. 2024; 15: 2129–2144. https://doi.org/10.21037/jgo-24-245

[16] Chen J, Liu QM, Du PC, Ning D, Mo J, Zhu HD, et al. Type-2 11β-hydroxysteroid dehydrogenase promotes the metastasis of colorectal cancer via the Fgfbp1-AKT pathway. American Journal of Cancer Research. 2020; 10: 662–673.

[17] Qi M, Fan S, Huang M, Pan J, Li Y, Miao Q, et al. Targeting FAPα-expressing hepatic stellate cells overcomes resistance to antiangiogenics in colorectal cancer liver metastasis mod-

els. The Journal of Clinical Investigation. 2022; 132: e157399. https://doi.org/10.1172/JCI157399

[18] Xia R, Hu C, Ye Y, Zhang X, Li T, He R, et al. HNF1A regulates oxaliplatin resistance in pancreatic cancer by targeting 53BP1. International Journal of Oncology. 2023; 62: 45. https://doi.org/10.3892/ijo.2023.5493

[19] Fu Q, Huang Y, Ge C, Li Z, Tian H, Li Q, et al. SHIP1 inhibits cell growth, migration, and invasion in non-small cell lung cancer through the PI3K/AKT pathway. Oncology Reports. 2019. https://doi.org/10.3892/or.2019.6990

[20] Leiphrakpam PD, Are C. PI3K/Akt/mTOR Signaling Pathway as a Target for Colorectal Cancer Treatment. International Journal of Molecular Sciences. 2024; 25: 3178. https://doi.org/10.3390/ijms25063178

[21] Afolabi HA, Salleh SM, Zakaria Z, Seng CE, Nafi SNM, Aziz AABA, et al. Molecular characterization of colorectal cancer (CRC) using next generation sequencing (NGS) in bridging the gap between research and clinical practice: from biomarker discovery to clinical implementation. Discover Oncology. 2025; 16: 268. https://doi.org/10.1007/s12672-025-01960-2

[22] Kassem NM, Seadawy MG, Gaafar M, Kassem HA, Ahmed Hussein AF, Ali Rizk EM, et al. Identifying actionable genetic mutations and microsatellite instability in liquid biopsy of colorectal cancer. Journal, Genetic Engineering & Biotechnology. 2025; 23: 100580. https://doi.org/10.1016/j.jgeb.2025.100580

[23] Li K, Wu X, Li Y, Hu TT, Wang W, Gonzalez FJ, et al. AKAP12 promotes cancer stem cell-like phenotypes and activates STAT3 in colorectal cancer. Clinical and Translational Oncology. 2023; 25: 3263–3276. https://doi.org/10.1007/s12094-023-03230-5

[24] Liao S, Yang Y, Chen S, Bi Y, Huang Q, Wei Z, et al. IL-24 inhibits endometrial cancer cell proliferation by promoting apoptosis through the mitochondrial intrinsic signaling pathway. Biomedicine & Pharmacotherapy = Biomedecine & Pharmacotherapie. 2020; 124: 109831. https://doi.org/10.1016/j.biopha.2020.109831

[25] Long M, Ouyang Q, Wen J, Zeng X, Xu Z, Zhong S, et al. DIRAS1 Drives Oxaliplatin Resistance in Colorectal Cancer via PHB1-Mediated Mitochondrial Homeostasis. Biology. 2025; 14: 819. https://doi.org/10.3390/biology14070819

[26] Xu J, Ji L, Ruan Y, Wan Z, Lin Z, Xia S, et al. UBQLN1 mediates sorafenib resistance through regulating mitochondrial biogenesis and ROS homeostasis by targeting PGC1β in hepatocellular carcinoma. Signal Transduction and Targeted Therapy. 2021; 6: 190. https://doi.org/10.1038/s41392-021-00594-4

[27] Wang X, Xu Z, Wang J, Wu C, Zhang L, Qian C, et al. A Mitochondria-Targeted Biomimetic Nanomedicine Capable of Reversing Drug Resistance in Colorectal Cancer Through Mitochondrial Dysfunction. Advanced Science. 2025; 12: 2410630. https://doi.org/10.1002/advs.202410630